Integrated Design of Structures

O. Sensburg,* G. Schmidinger, † and K. Füllhas‡
Messerschmitt-Bölkow-Blohm GmbH, Munich, Federal Republic of Germany

For highly sophisticated, subsonically unstable fighter airplanes flying supersonically, a joint strategy to lay out the flight control system restricting design loads must be adopted. Such a strategy does not sacrifice performance since the majority of performance-critical design cases are not load critical. A carefree maneuvering control system limits design parameters (accelerations, acceleration rates, velocities, attitudes) in such a way that design loads are not exceeded. The design loads are defined in an interdisciplinary approach between flight control systems designers, loads engineers, and aeroelasticians. To minimize wave drag supersonically requires low thickness-to-chord ratios on surfaces and, hence, gives considerable static aeroelastic effects at high dynamic pressures. Control surface geometry cannot be selected using rigid aerodynamic derivatives as in the past, since this will lead to high structural mass penalties as well as too large hydraulic actuators requiring increased power supply. Therefore, this geometry must be found by applying modern structural optimization algorithms that deliver the exchange rate between structural weight penalties and the required hydraulic power, which is a function of control surface efficiency. The higher the actuator area is to produce high forces at load critical cases, the higher is the volume at low dynamic pressures where large deflections with high rates of all control surface are required. This gives the design case for the hydraulic pump and engine power takeoff. The interdisciplinary design method as applied to a modern fighter aircraft is described in this paper.

Nomeclature

$\frac{c_{L_\xi \text{flex}}}{c_{L_\xi \text{rigid}}}$	= roll efficiency
flap I	= $t_{ib} = 15\%$; $t_{tb} = 30\%$
flap II	= $t_{ib} = 15\%$; $t_{ob} = 40\%$
g	= normal load factor
H/M_{TE}	= hinge moment of trailing-edge flap
Ma	= Mach number
$N_{F/P}$	= normal force of foreplane
n_y	= lateral load factor
n_z	= normal load factor
p	= roll rate
$\dot{p}$	= roll acceleration
$\dot{q}$	= pitch acceleration
R/M	= rolling moment
r	= yaw rate
$\dot{r}$	= yaw acceleration
TSO	= aeroelastic tailoring and structural optimization
t	= time
t_{ib}	= inboard flap chord, %
t_{ob}	= outboard flap chord, %
η_{TE}	= trailing-edge flap deflection
$\eta_{F/P}$	= foreplane deflection
φ	= bank angle
θ	= ply orientation

Introduction

AN integrated structural design procedure was always applied in the past to produce lightweight aircraft structures. The method used was largely dependent on the experience and creativeness of the chief designer. For modern, naturally unstable airplanes with carbon fiber structures flying at supersonic speeds, the application of detailed structural finite-element models, early simulation results using flight control system (FCS) characteristics and "elastified" derivatives, and tuning the FCS to minimize loads while still respecting performance requirements is mandatory in the preliminary design stage. A finite-element optimization algorithm for carbon fiber materials has been set up at Messerschmitt-Bölkow-Blohm (MBB).[1,2] In this method, strength and static aeroelastic efficiency requirements[3] are fulfilled simultaneously with minimum structural weight. The application of such a program is absolutely necessary to achieve the described goals. This paper describes how aerodynamic loads are determined, how dependent they may be on FCS design, and how aeroelastic tailoring[4] is applied together with geometrical parametric studies to achieve maximum roll rates with minimum structural weight and minimum installed hydraulic power.

Carefree Handling and Maneuver Load Control

A flight control system for a naturally unstable aircraft[5] will drive design parameters (accelerations, acceleration rates, velocities, attitudes) in an optimal way to fulfill its required maneuver performance. Additionally, the FCS must respect parameter envelopes so that no design loads are exceeded.[6] These design loads are defined in an iterative process between the FCS designers, load engineers, and aeroelasticians. A few examples of how this is performed and how load envelopes are produced in the following.

A fighter aircraft is presented in Fig. 1. Its primary control surfaces are the inboard flaperons, outboard flaperons, foreplane, and rudder. The inboard/outboard flaperons and/or foreplane can therefore be used for trimming and controlling the longitudinal aircraft motion. It depends on the allocation of stick inputs to these control surfaces.

Figure 2 shows an example of how much the foreplane and wing trailing-edge flap can be affected by an appropriate choice of the initial trim contribution. This applies for the subsonic region where the aircraft is unstable longitudinally, as well as for the supersonic region where the aircraft is stable.

It is interesting to note that the aircraft needs only small control deflection angles for initiation of a maneuver, as expected, but that the control deflection has to be checked immediately in order to stop the effect of instability. Therefore,

Received July 2, 1986; revision received July 21, 1988.

*Chief, Project Structures. Member AIAA.
†Head, Project Structural Technology, Airplane Division.
‡Head, Project Loads, Airplane Division.

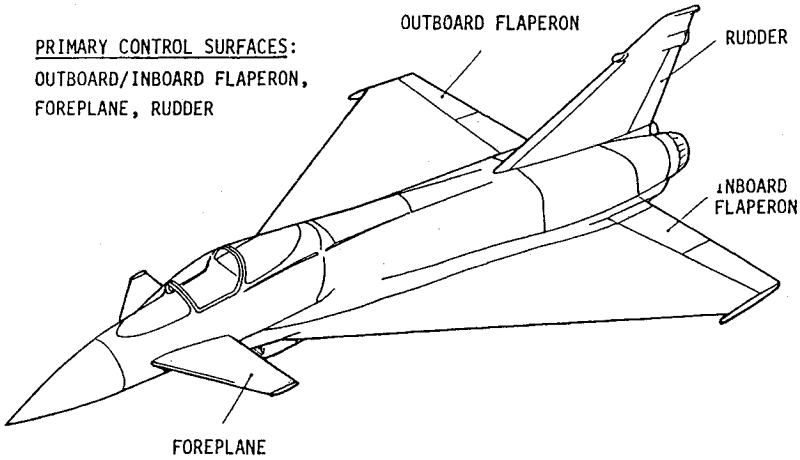

Fig. 1 Aircraft control surfaces.

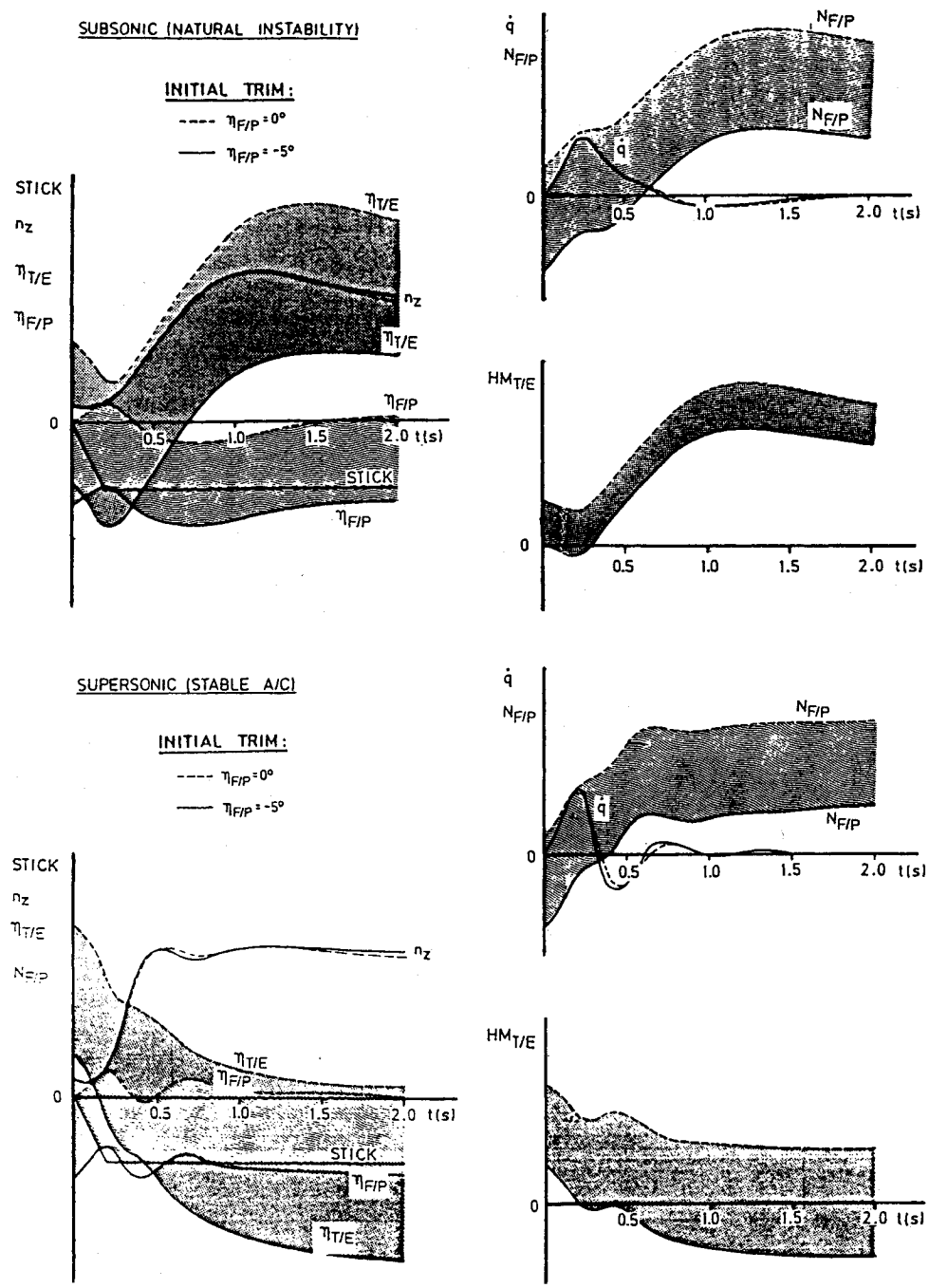

Fig. 2 Adaption of trim control for load optimization.

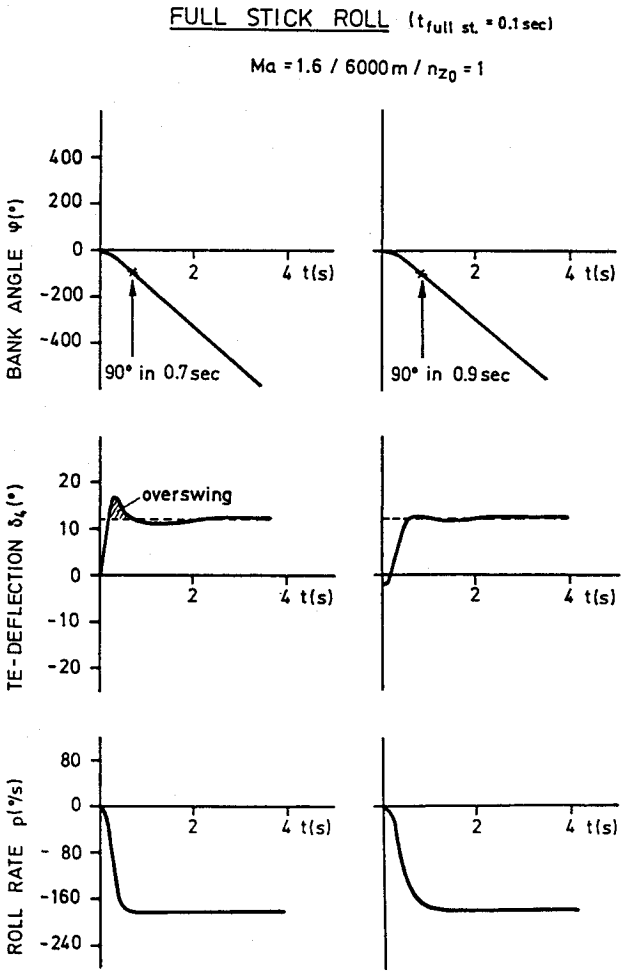

Fig. 3 Adaption of control system in order to achieve 36% load reduction (trailing-edge flap).

no similarity between stick input and actual control surface deflections can be seen subsonically, while supersonically the usual increasing control deflection is seen in order to command a steady maximum g condition.

If the foreplane/flap schedule is chosen only from a handling and performance point of view, one may run into problems with the design loads on both surfaces. Advantages on both surfaces are found by choosing an optimum loads concept.

It must be emphasized that in designing the control system it is very important to feed in the design loads aspects at a very early stage, as can be explained by Fig. 3. It may be accepted from a handling/performance point of view to overfulfill the time-to-bank requirement by an overswinging control deflection. This clearly increases the control hinge moments and the load reductions are achieved—in this case about 36%—by adopting the maximum acceptable time to bank.

Real-time simulations with measured aerodynamic derivatives, aeroelastic efficiencies, and optimized control laws must be performed and maximum response parameters selected from time histories. Then, the actual design loads can be derived.

These examples clearly illustrate that the aerodynamic loads produced by manuevers depend on carefully chosen control laws/trim programs of the FCS.

Static Aeroelastic Considerations

Aeroelastic efficiencies of control surfaces can show large reductions vs airspeed and Mach number[7] (Fig. 4). They must be carefully chosen so that not too many iterative steps are

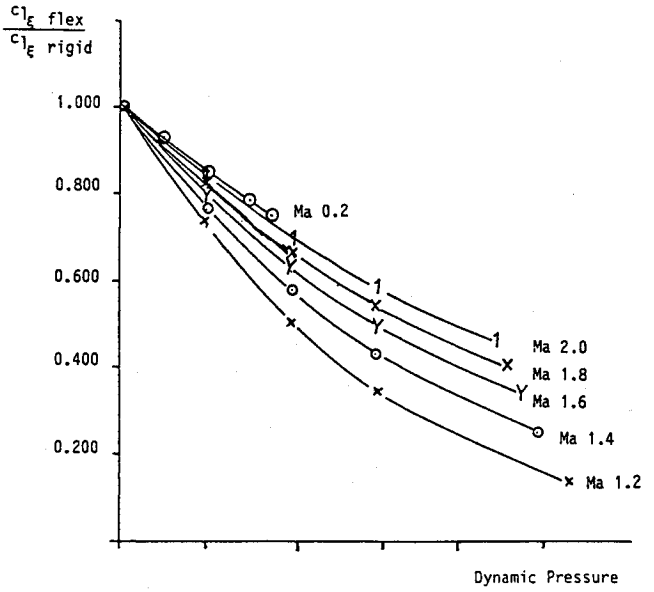

Fig. 4 Aeroelastic correction factor for role efficiency of outboard trailing-edge flap.

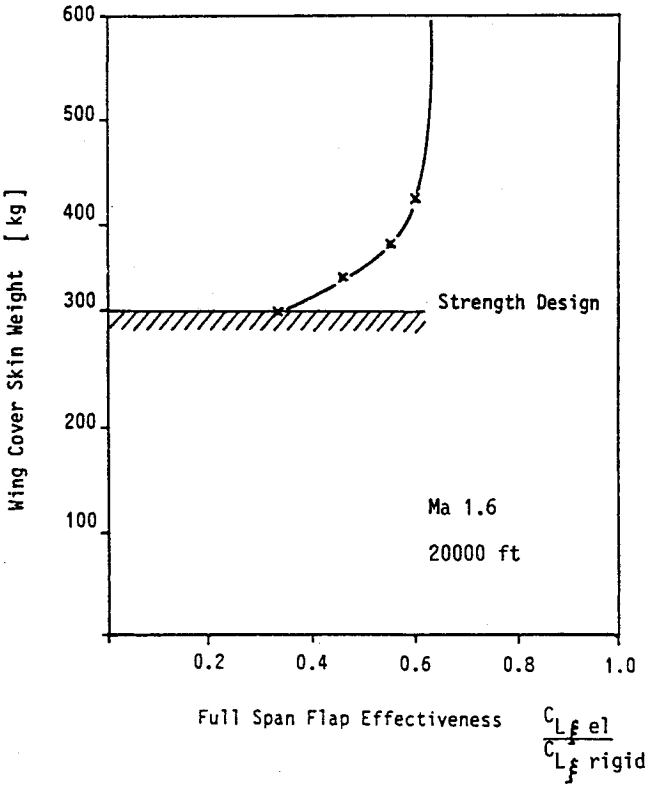

Fig. 5 Required structural weight for increasing elastic flap effectiveness requirements.

necessary and also so that the structural weight needed to fulfill certain efficiency requirements is not prohibitive (Fig. 5).

The strong influence of the aircraft elastic structure on aerodynamic loading is shown in Fig. 6.

An approach to achieving high sustained roll rates at high dynamic pressures with aeroelastic tailoring of a carbon fiber wing, while minimizing hinge moment demand and therefore hydraulic power and flow requirements, is as follows:

A certain roll rate was chosen as the design aim at *Ma* 1.6 and 20,000 ft, high enough to make the aircraft agile and competitive. All calculations were performed with the TSO computer program[8] with a MBB-modified optimization algo-

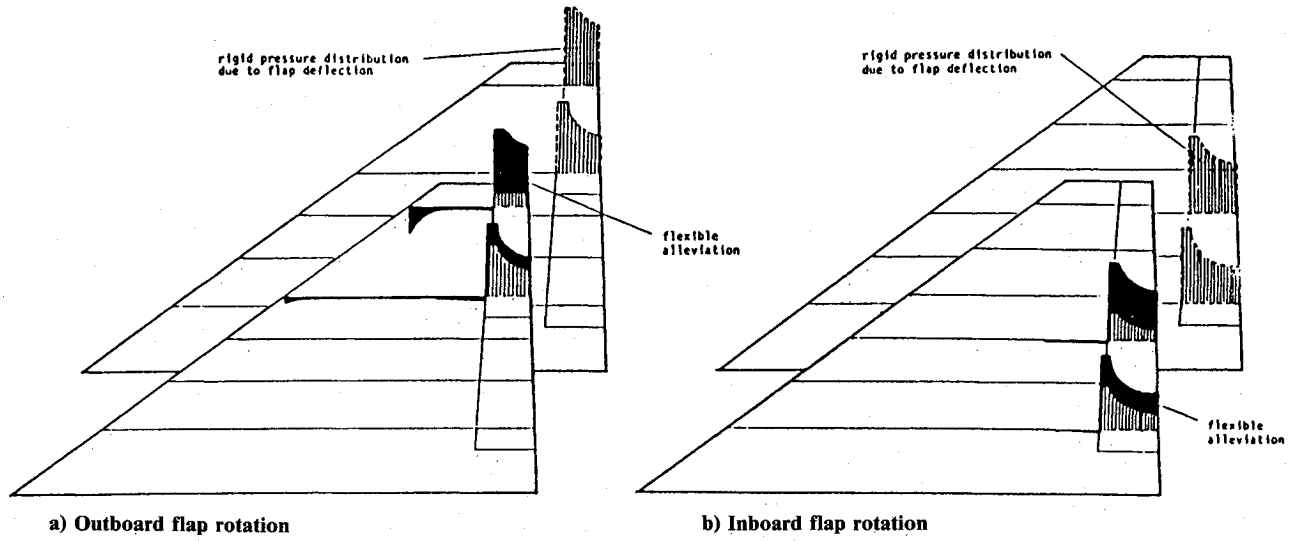

a) Outboard flap rotation b) Inboard flap rotation

Fig. 6 Elastic pressure distribution (Mach 1.2, sea level).

rithm. The program can minimize the structural weight by proper laying of carbon fiber composite (CFC) laminates in direction and thickness, in this case simultaneously fulfilling static strength and efficiency (stiffness) requirements. Because a plate model is used for structural representation, quick changes in geometry (i.e., flap size) are possible that are very time consuming on a finite-element model. On the other hand, there is a certain loss of accuracy, so the results should be taken as tendencies rather than fixed values of structural weight.

The aim of the exercise was to optimize the CFC wing laminates (with respects to weight) in thickness and direction, while always fulfilling the roll rate required, in such a way that the lowest trailing-edge hinge moments could be found. Flap size (chord and length) were varied parametrically. An estimate of the exchange rate of trailing-edge hinge moments with weights is given in Fig. 7. This figure shows that halving the necessary hinge moments can save about 85 kg weight on trailing-edge flaps, actuator, and hydraulics.

Search for Optimum Trailing-Edge Size

Due to strong influences of elastic deformations on stationary aerodynamic forces at high dynamic pressures, the classical aerodynamic approach using rigid derivatives must be replaced by a method that optimizes the structural weight fulfilling the roll requirement. It should be emphasized that all parametric investigations must be done by optimizing the structure for every point investigated, which can mean different laminate thicknesses and directions for each point. A study taking an optimized structure for one point and analyzing another point could be misleading.

The exercise was conducted in two steps: 1) find the maximum possible chord flap, and 2) define a split line for two flaps.

The scope of the study is shown in Fig. 8. Different inboard flap chords were not investigated because the requirement was also to obtain the largest chord flap possible aeroelastically to assure controllability at high subsonic Mach numbers, where longitudinal static instability is highest and the flap angle may be restrictive. In order to have maximum possible flap travel available, it is necessary to do most of the required trimming with the foreplane.

Results

Figure 9 shows the hinge moment and flap angle requirement to fulfill the roll requirement for flap I (Fig. 8). It shows a steep weight gradient for hinge moment reduction near the

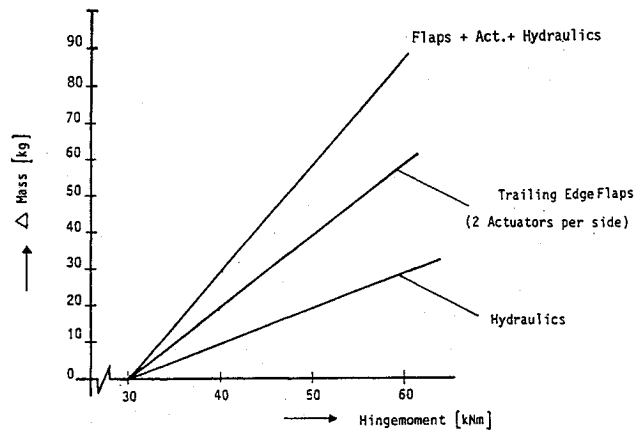

Fig. 7 Added mass as a function of trailing-edge hinge moment.

strength design, which flattens considerably at 40 kN·m. Flap deflection shows similar behavior. It should be noted that the flap deflection for the rigid wing cannot be reached physically with the given t/c ratio and material properties. In this investigation, rigid flap means one that is continuously driven and has no flexibility of its own. Two optimization runs were made with the flexible flap driven at two spanwise positions (0.2 and 0.5 wing span) that showed the flap angle goes up, whereas the hinge moment goes down. Figure 10 presents results for flap II (40% outboard chord). The behavior of hinge moment and flap angle is similar, but 40 kN·m can be reached with less structural weight. When the flexible flap was introduced, the flap angle went up considerably, whereas the hinge moment was reduced only near the strength design.

A boundary for increasing the flap chord outboard is the flutter speed[9] with a tip missile attached and the request for a reasonable torsional box to get a high enough missile attachment stiffness. As a matter of interest, flutter speeds of the clean wing were calculated and are presented in Fig. 11. From this figure, it can be deduced that for the clean wing there is no difference between wing with flap I or II. The flutter speed in-

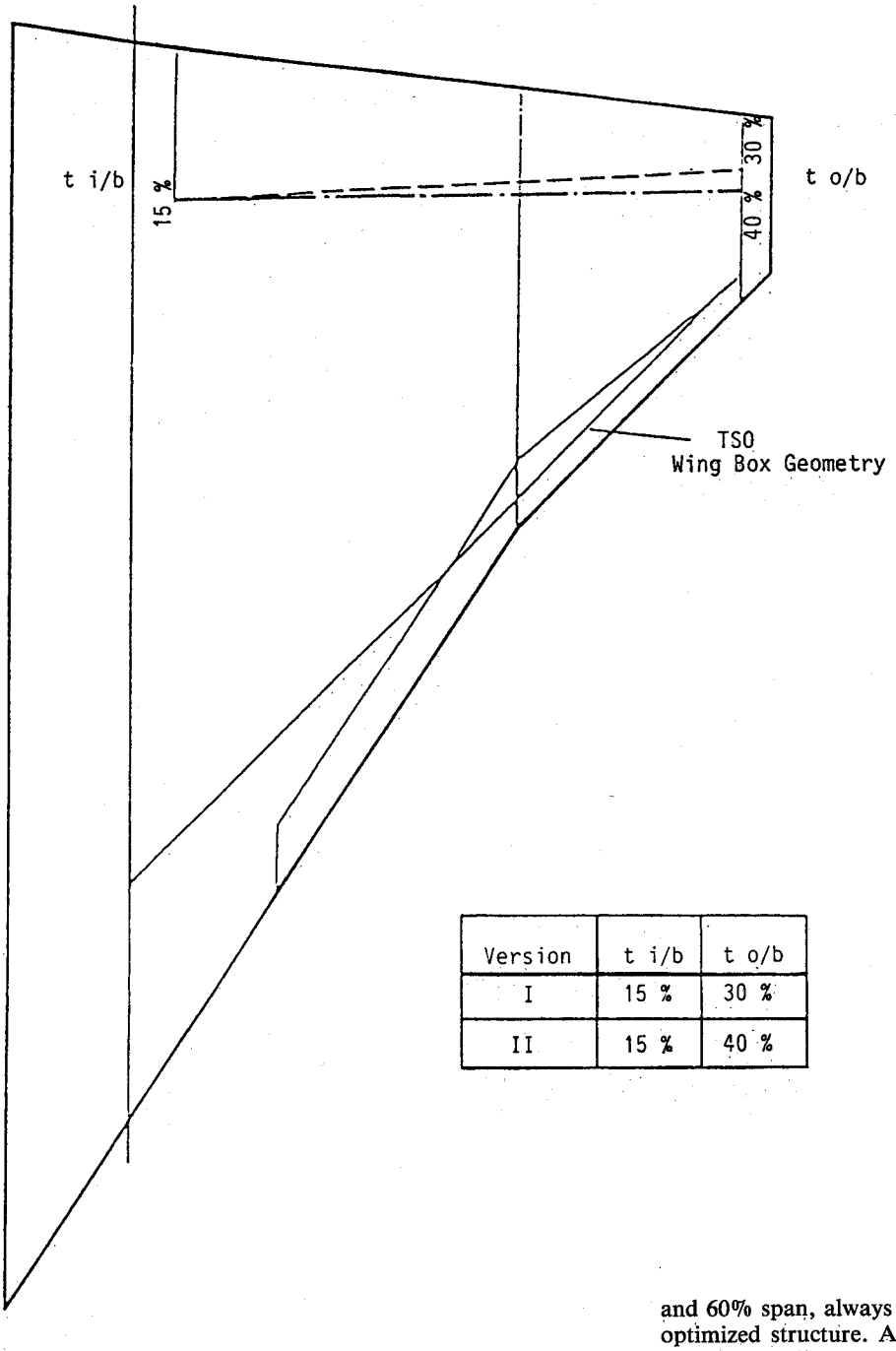

Version	t i/b	t o/b
I	15 %	30 %
II	15 %	40 %

Fig. 8 Flap geometry.

creased with structural weight because the torsion frequency goes up. In Fig. 12, *v-g* plots and vibration modes for one case are presented.

In Fig. 13, the added mass (above the mass for strength design) as a function of the hinge moment is plotted (from Figs. 9 and 10) and the weight reduction as function of hinge moment (from Fig. 7). The optimum hinge moment is about 45 kN·m for a full span flap with a mass saving of 20 kg for flap I. The larger chord outboard flap II was chosen for further investigation, because it clearly shows a greater total mass reduction vs flap I with a hinge moment of about 45 kN·m.

Flap Split Definition

A full span flap is not possible for two reasons: 1) the FCS redundancy philosophy is not fulfilled, and 2) high internal structural forces are induced into the wing and flap. The minimum of two flaps per side was chosen because all requirements, including maneuver load control, could be fulfilled with such an arrangement.

In order to define the flap split spanwise, two exercises were performed. The full span flap was cut outboard down to 80 and 60% span, always fulfilling the roll requirement with an optimized structure. As shown in Fig. 14, this is the wrong way to go. Hinge moment and flap deflection increase above values of 45 kN·m and 15 deg (where $C_{L\eta}$ becomes nonlinear) and cannot be reduced by added mass because the weight gradients are too flat.

In Fig. 15, the full span flap is cut to 80% and 54% span. The hinge moment goes down now, but the deflection becomes marginal (close to 15 deg) when a 54% outboard span flap is used alone to fulfill the roll requirement. Load introduction with 30 kN·m at such a far outboard position as 54% becomes extremely difficult. Figure 16 shows clearly that the optimum lies below a 40 kN·m installed hinge moment, which is lower than for full span flap (see Fig. 13).

From Fig. 16 and Table 1, it can be deduced that it is best to use maximum deflection from outboard flap. Thus,

$$\text{Ratio of } \frac{\text{flexible hinge moment}}{\text{flexible wing roll moment}}$$

is

1.5 × better than full flap
2 × better than inboard flap

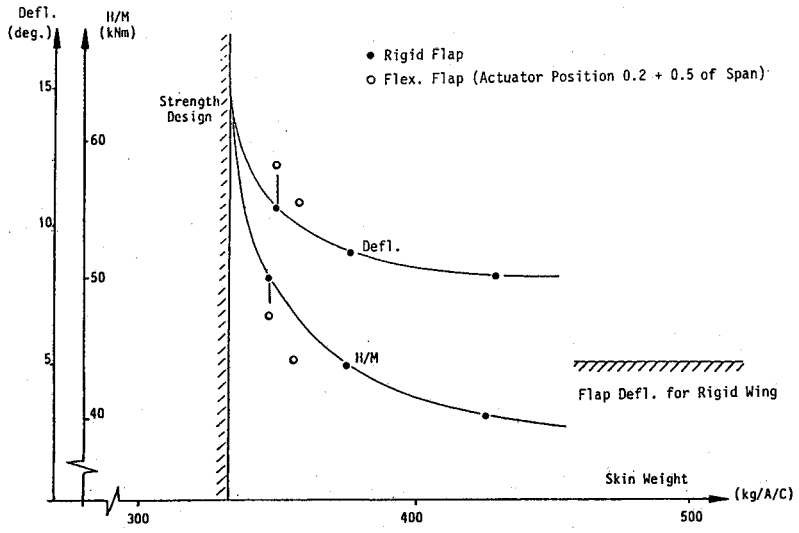

Fig. 9 Deflection and hinge moment for flap I (Mach 1.6, 20,000 ft).

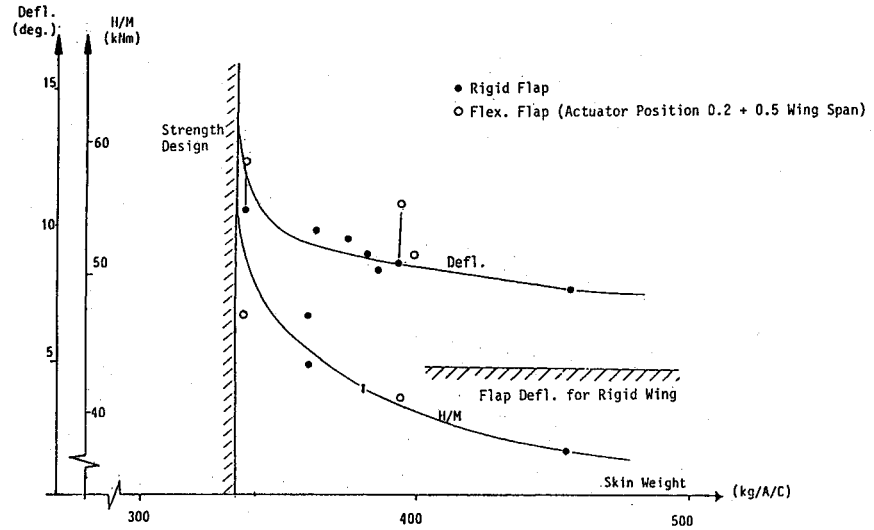

Fig. 10 Deflection and hinge moment for flap II (Mach 1.6, 20,000 ft).

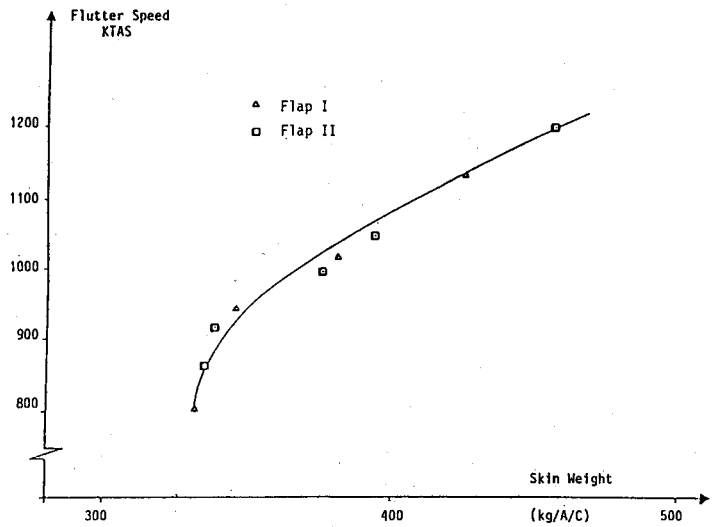

Fig. 11 Flutter speed vs skin weight.

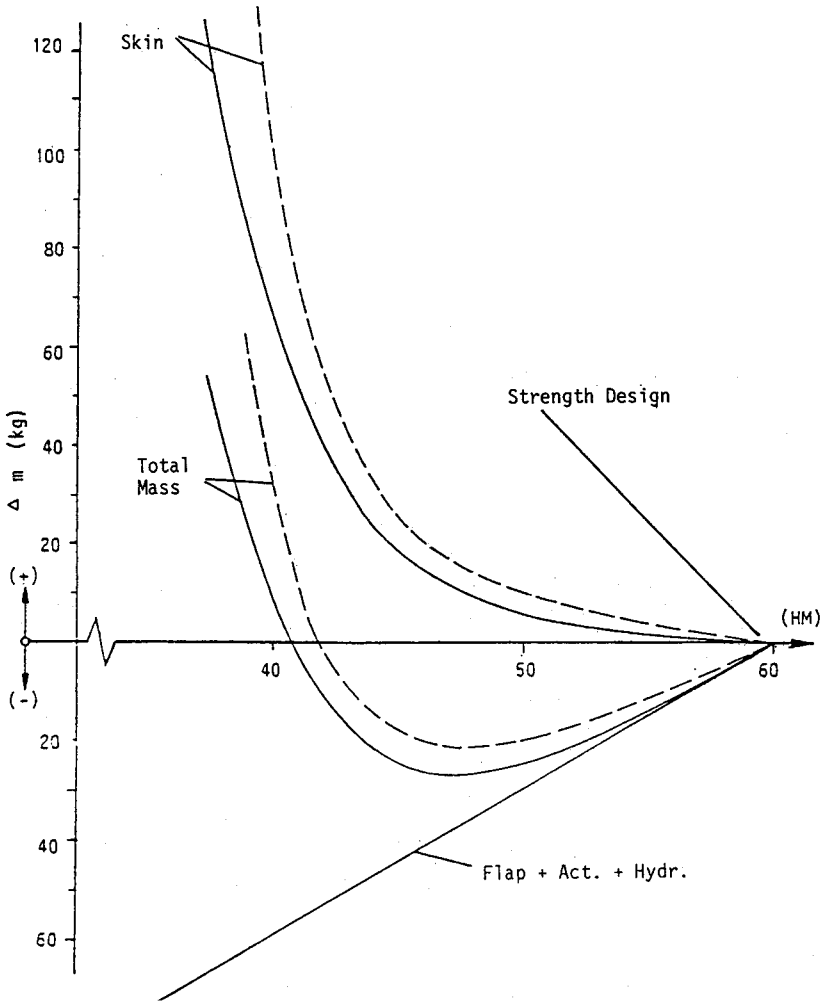

Fig. 12 Flap II *v-g* plot and vibration modes.

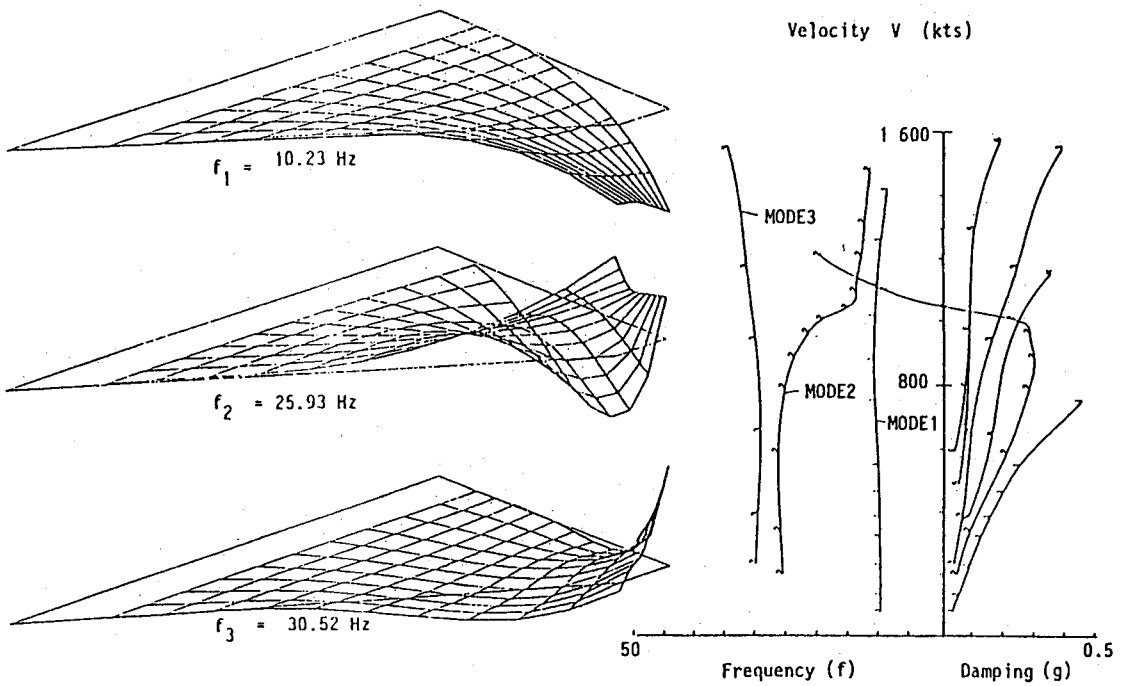

Fig. 13 Added mass as a function of hinge moment.

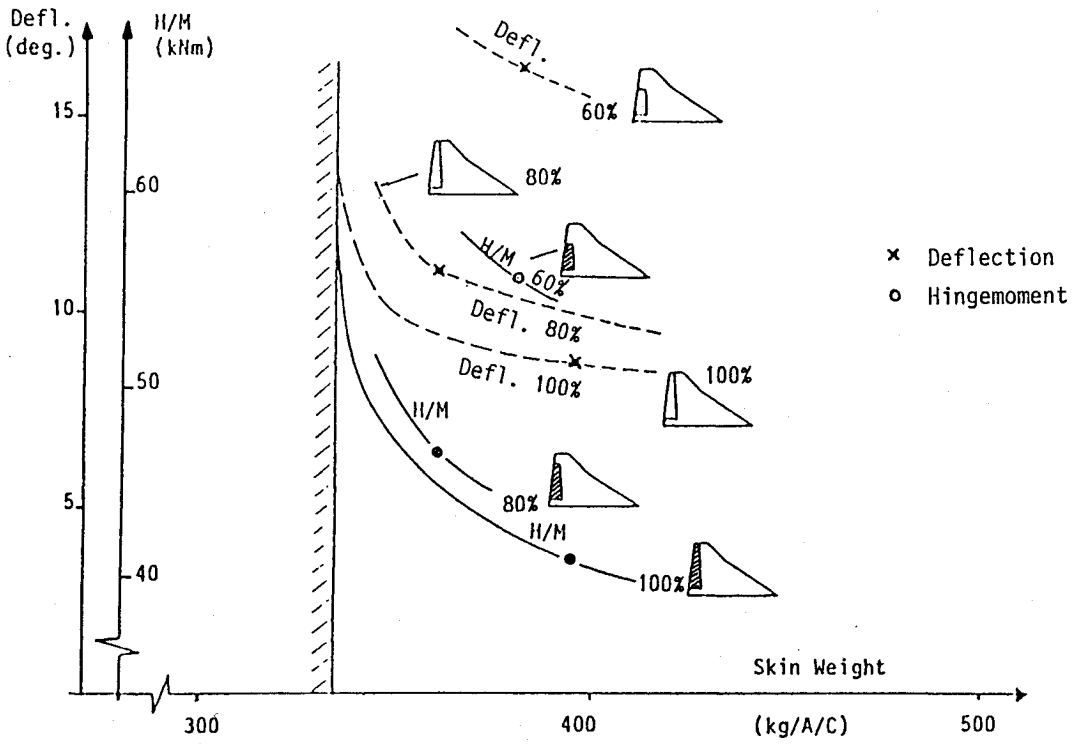

Fig. 14 Deflection and hinge moment for outboard flap II vs skin weight (various flap geometries).

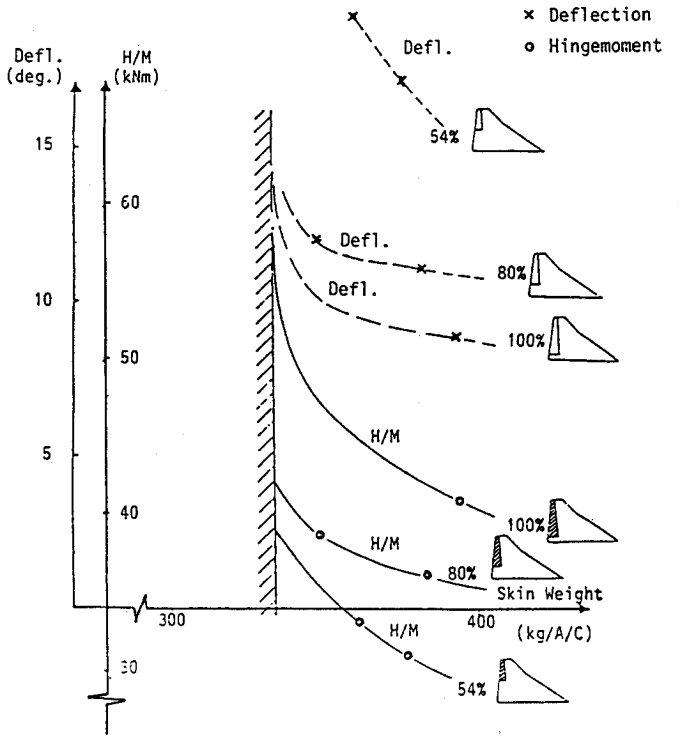

Fig. 15 Deflection and hinge moment of outboard flap II vs skin weight (various flap geometries).

A viable load introduction limit of 22 kN·m and 15 deg flap angle must not be violated.

Therefore, the inboard flap must also be employed because an outboard flap alone cannot stay within these limits and fulfill the given roll requirement. The hinge moments vs deflections of inboard and outboard flaps are shown in Fig. 17.

Proposed Flap Split

The following conditions must be fulfilled:

1) Use the largest possible outboard span flap with maximum angle of 15 deg.

2) Do not exceed 22 kN·m with an outboard flap.

The two cases calculated (without changing the aerodynamic grid) are shown in Fig. 18. A split of 50% inboard and 50% outboard flap results. With a linear interpolation of the Fig. 18 results, this would give an outboard hinge moment of 22 kN·m and a total of 34.4 kN·m.

CFC Wing Layer Thickness and Directions

The wing cover skin thickness distributions for the selected case are shown in Fig. 19. Isothickness lines for three fiber orientations are plotted in increments of one ply (0.005 in.) or multiples. For these designs, a total of three different fiber directions had been preselected. It would have been possible to optimize their orientations individually. But in our case, they were allowed only to rotate together as a set with constant angles of +45 deg between them (at every total angle the three layers have optimum thicknesses). This is a common approach because the most theoretical as well as experimental material data exist for this family of laminates (0 deg, ±45 deg, 90 deg). the influence of the fourth layer (90 deg plies) was neglected in this study because its portion of the total laminate usually lies between 10 and 15%.

Compared to most state-of-the-art carbon fiber designs, the global and local amounts +45 deg and −45 deg plies are unbalanced in Fig. 19. This additional design feature would be less important for a pure strength design (with almost symmetrical load distribution in the spanwise direction). But an aeroelastic flap effectiveness requirement, with loads being introduced into the wing torsion box through the flap asymmetrically, favors an unbalanced laminate composition. This will result in thickness distributions that give high stiffness in one direction and reduced stiffness in the other perpendicular to the first one. Interesting to note that layer 1 ($\theta = 27.88$ deg) increases outboard in thickness.

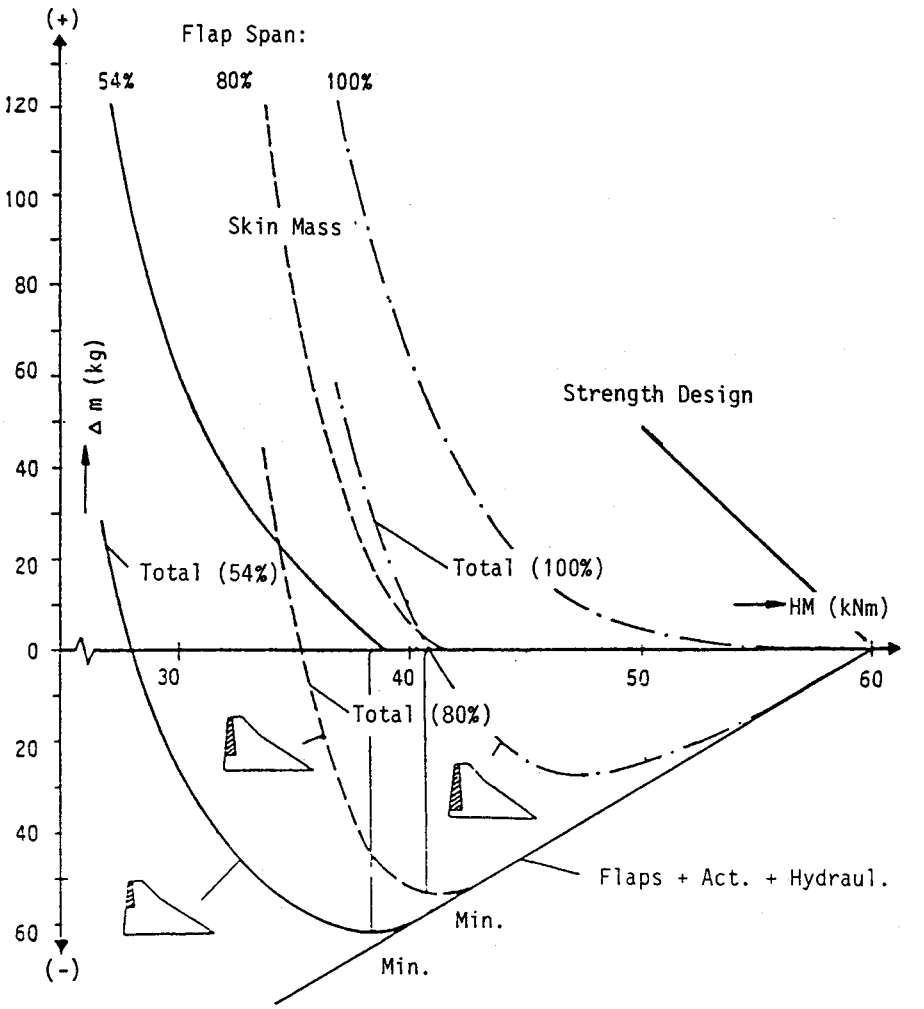

Fig. 16 Added mass as a function of hinge moment for various outboard flap spans.

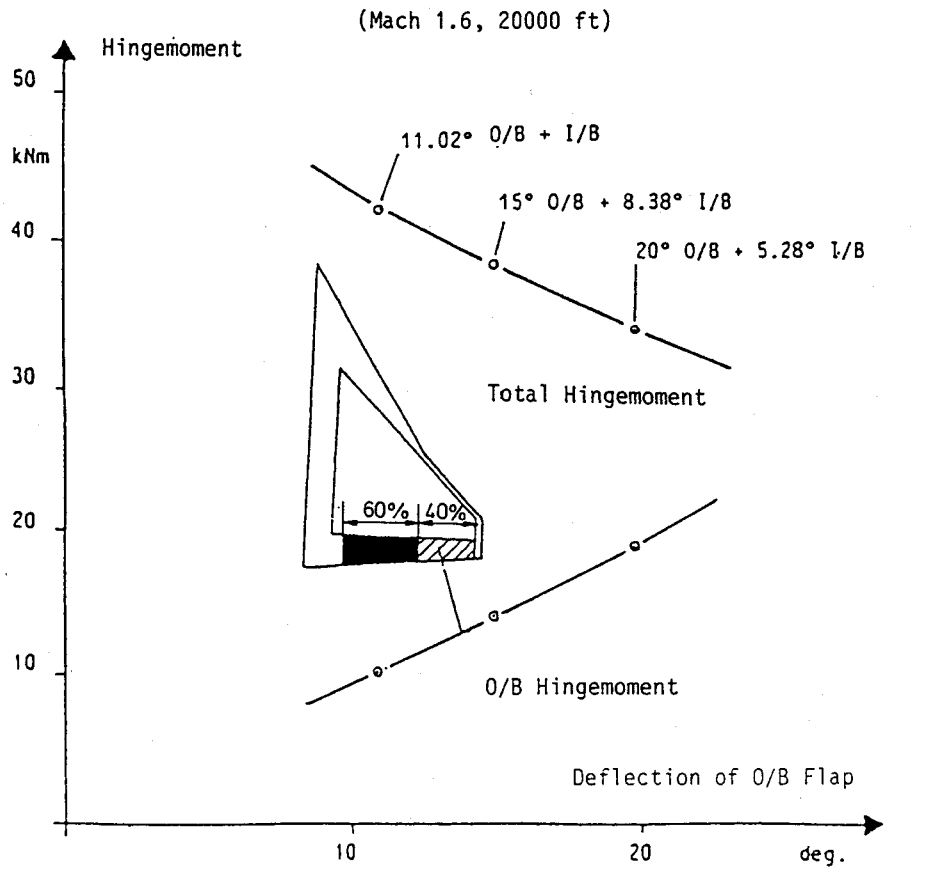

Fig. 17 Hinge moments vs deflections of inboard/outboard flaps.

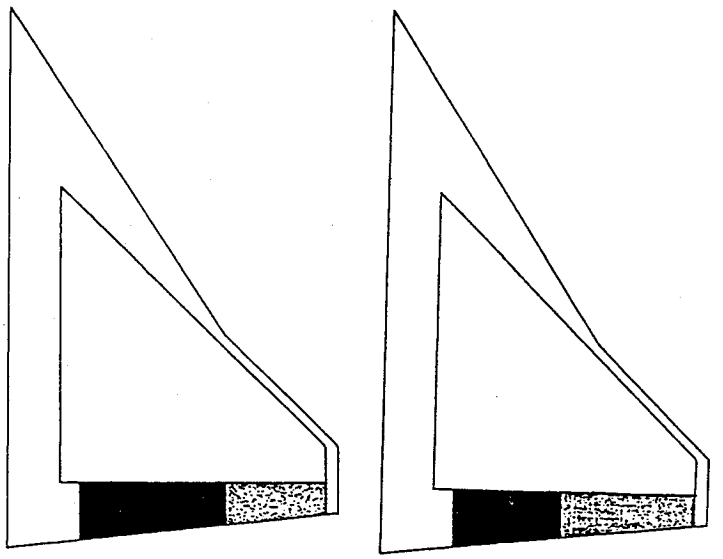

Fig. 18 Hinge moments for two different flap splits.

Percentage Flaperon	60%	40%	46%	54%
Flap angle (IB/OB)	6.23°	15°	3.5°	15°
Hinge-Moment (IB/OB) (kNm)	23.8	14.0	8.38	24.98
Total Hinge Moment (kNm)	37.8		33.4	

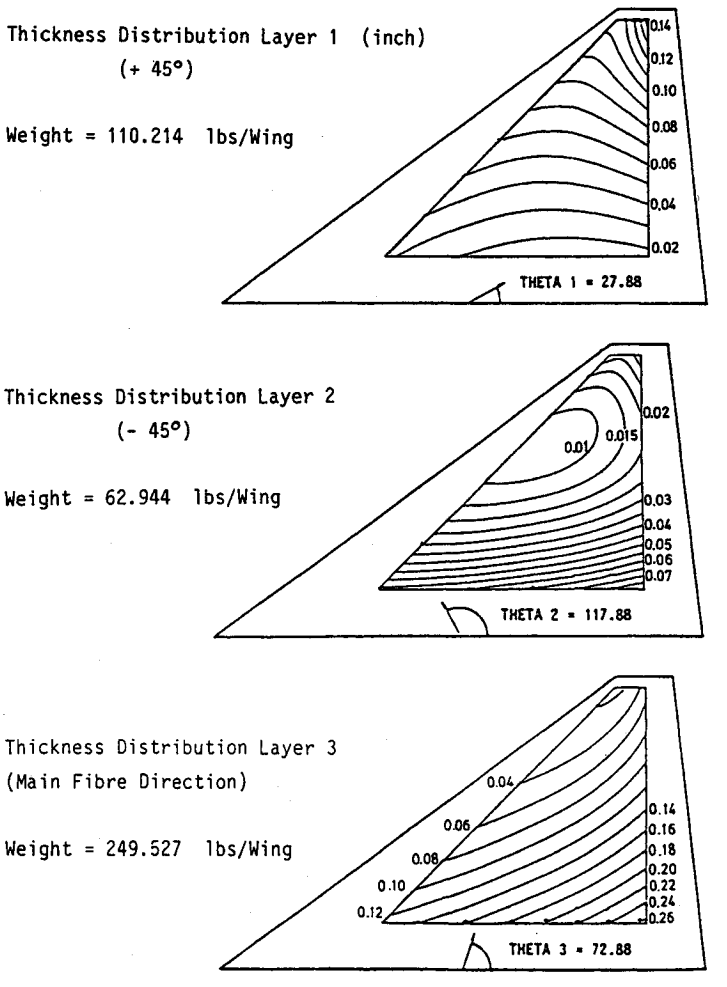

Fig. 19 Thickness distributions of three carbon fiber layers (0 deg, ±45 deg).

Table 1 Roll Efficiencies, flexibility corrections, and control angle of i/b and o/b flap (type II)

Flap	Full span, rigid	inboard only, rigid	outboard only, rigid	Full span, flex	inboard only, flex	outboard only flex
Rolling moment, rigid, kN·m/1 deg defl	42.3	22.3	20.2	42.3	22.3	20.0
Rolling moment, flex, kN·m/1 deg defl	22.5	13.7	8.8	18.5	11.5	7.0
Rolling moment efficiency	0.53	0.61	0.44	0.44	0.52	0.35
Hinge moment, rigid kN·m/1 deg defl	5.35	3.88	1.33	5.35	3.83	1.33
Hinge moment, flex, kN·m/1 deg defl	4.65	3.45	1.19	3.83	2.84	0.93
Hinge moment efficiency	0.87	0.89	0.90	0.72	0.74	0.70
$\frac{\text{Flex H/M}}{\text{Flex R/M}}$	0.21	0.25	0.14	0.21	0.25	0.13
Deflection for roll req	9.04	9.04	9.04	11.02	11.02	11.02
H/M for above deflection, kN·m	42.0	31.2	10.8	42.2	31.3	10.2

The 0 deg fiber direction ($\theta = 72.88$ deg) is used mainly to carry static loads and, for this reason, the thickness increases toward the root.

Compared to the unbalanced design, the balanced wing cover skins have an additional weight penalty of 60 kg per aircraft. Of course, the plies are balanced in both cases relative to a plane of symmetry in the center of upper and lower skins to avoid deformations and interlaminar stress without external loads.

Conclusions

It is extremely difficult to assess the result of an integrated design of structures as described here in an exact amount of total structural mass saved compared to a conventional design method, because only the new integrated method was applied.

Collecting all available information for this special case, a mass saving of approximately 5% of aircraft mass without fuel is estimated.

References

[1]Gödel, H., Hörnlein, H, Keppeler, D., and Sensburg, O., "Modern Trends in Aircraft Structural Design," AGARD Rept. No. 726, April 1986, pp. 1-1–1-8.

[2]Hörnlein, H., "Take-Off in Optimum Structural Design in Computer Aided Optimal Design: Structural and Mechanical Systems," Mota Soares, C. A. (ed.), *Ser. F: Computer and Systems Sciences*, Vol. 27, Springer-Verlag, Berlin-Heidelberg, 1987, pp. 901–919.

[3]Försching, H. W., "Grundlagen der Aeroelastik," Springer-Verlag, Berlin-Heidelberg, New York, 1974.

[4]Shirk, M. H., Hertz, T. J., and Weisshaar, T. A, "A Survey of Aeroelastic Tailoring-Theory, Practice, Promise," AIAA Paper 84-0982, May 1984.

[5]Sensburg, O. and Zimmerman, H., "Impact of Active Control on Structures Design Fighter Aircraft Design," AGARD CP-241, Oct. 1977.

[6]Sensburg, O., Bartsch, O., and Bergmann, H., "Reduction of the Ultimate Load Factor by Applying a Maximum Load Concept," *Journal of Aircraft*, Vol. 24, Nov. 1987, pp. 759–767.

[7]Schmidinger, G. and Sensburg, O., "Static Aeroelastic Considerations in the Definition of Design Loads for Fighter Airplanes," *Proceedings of 63rd Meeting of SMP of AGARD*, AGARD Pub. 274, Sept. 1986.

[8]Lynch, R. W., Rogers, W. A., Braymen, W. W., Hertz, T. J., "Aeroelastic Tailoring of Advanced Composite Structures for Military Aircraft," Air Force Flight Dynamics Lab., TR-76-100, 1976.

[9]Schweiger, J., Sensburg, O., and Ponzi, C., "Aeroelastic Tailoring for Flutter Constraints," ICAS 86-4.7.1, Sept 1986.